SUPPLEMENTAL INFORMATION

Atomic view of the HIV-1 Matrix lattice. Implications on virus assembly and Env incorporation

Alexandra B. Samal, Todd J. Green, and Jamil S. Saad*

Department of Microbiology, University of Alabama at Birmingham, Birmingham, AL 35294

Corresponding Author: Jamil S. Saad, Ph.D.
Department of Microbiology
University of Alabama at Birmingham
845 19th Street South, Birmingham, AL 35294
Phone: (205)-996-9282
Fax: (205)-996-4008

Email: saad@uab.edu

Table S1. X-Ray Crystallographic Data Collection and Model Refinement

Parameter	
Wavelength (Å)	
Resolution range	24.9 - 2.15 (2.228 - 2.15)
Space group	R 3 2 :H
Unit cell (Å)	96.56 96.56 216.91 90 90 120
Total reflections	130208 (12029)
Unique reflections	21434 (2087)
Multiplicity	6.1 (5.8)
Completeness (%)	99.61 (98.86)
Mean I/sigma(I)	21.66 (2.64)
Wilson B-factor	43.02
R-merge	0.04682 (0.5734)
R-meas	0.05124 (0.6327)
R-pim	0.02045 (0.2634)
CC1/2	0.999 (0.805)
CC*	1 (0.945)
Reflections used in refinement	21429 (2088)
Reflections used for R-free	1996 (192)
R-work	0.183 (0.2700)
R-free	0.236 (0.3500)
CC(work)	0.968 (0.862)
CC(free)	0.953 (0.723)
Number of non-hydrogen atoms	2641
macromolecules	2480
ligands	77
solvent	84
Protein residues	308
RMS(bonds)[a]	0.007
RMS(angles)	0.83
Ramachandran favored (%)	98.01
Ramachandran allowed (%)	1.99
Ramachandran outliers (%)	0.00
Rotamer outliers (%)	4.44
Clashscore	5.45
Average B-factor	66.27
macromolecules	65.80
ligands	87.59
solvent	60.60
Number of TLS groups	24

Statistics for the highest-resolution shell are shown in parentheses.
[a] RMS, root mean square.

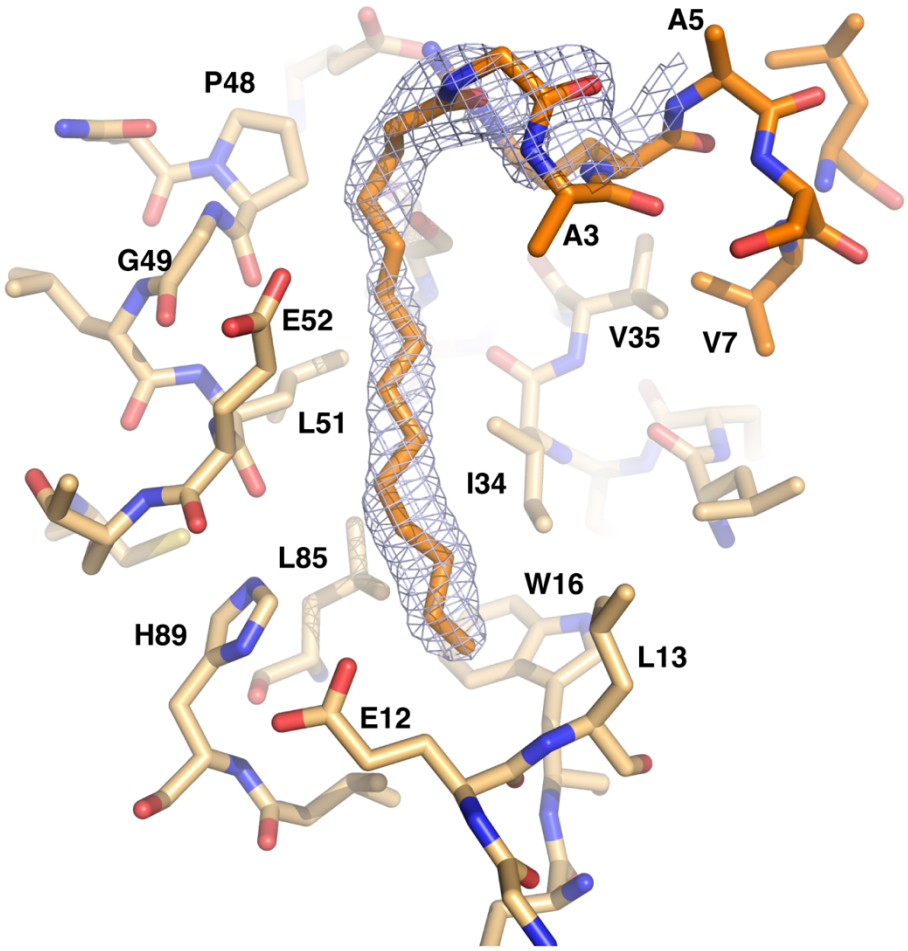

Figure S1. Close-up view of the myr group and the hydrophobic pocket. Portions of two myrMA$_{112}$ monomers (chain **b**) are shown with orange and light orange carbon backbone, respectively. Electron density (2Fo-Fc, contour level: 1.0σ) is shown surrounding the myr group.

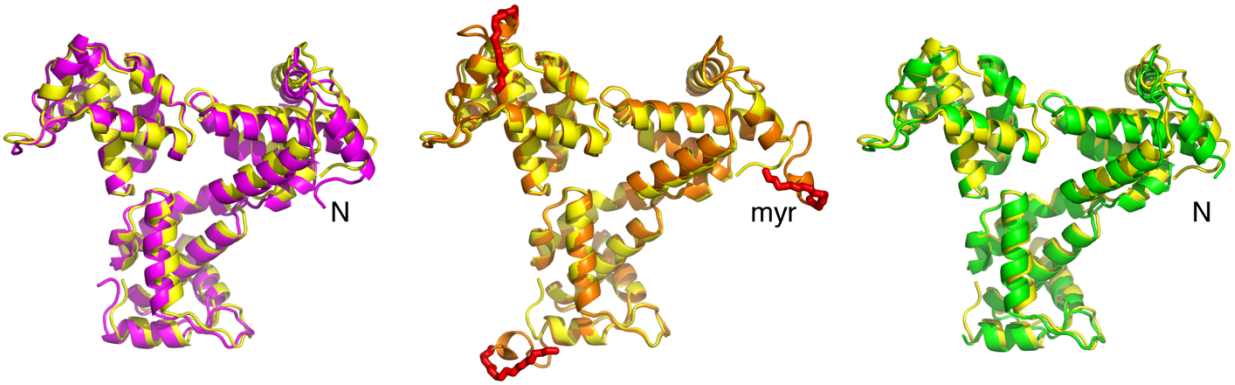

Figure S2. Comparison of the X-ray structures of HIV-1 myrMA$_{112}$ and WT myr(–)MA. The asymmetric unit of the crystal structure of HIV-1 myrMA$_{112}$ contained three copies (chains **a**, **b**, and **c**). Application of crystallographic symmetry revealed three independent trimeric assemblies (chain **a**, magenta; chain **b**, orange; chain **c**, green). Trimers formed by the three independent chains are overlayed on the trimer structure of the WT myr(–)MA protein (yellow; PDB ID: 1HIW) (1). The myr group in chain **b** is shown as red stick. For chains **a** and **c**, the electron density for the myr group as well as residues 2-5 and 2-9, respectively, were not observed likely due to a highly flexible conformation. The structure of the myrMA$_{112}$ protein and the trimer arrangement are very similar to the WT myr(–)MA protein.

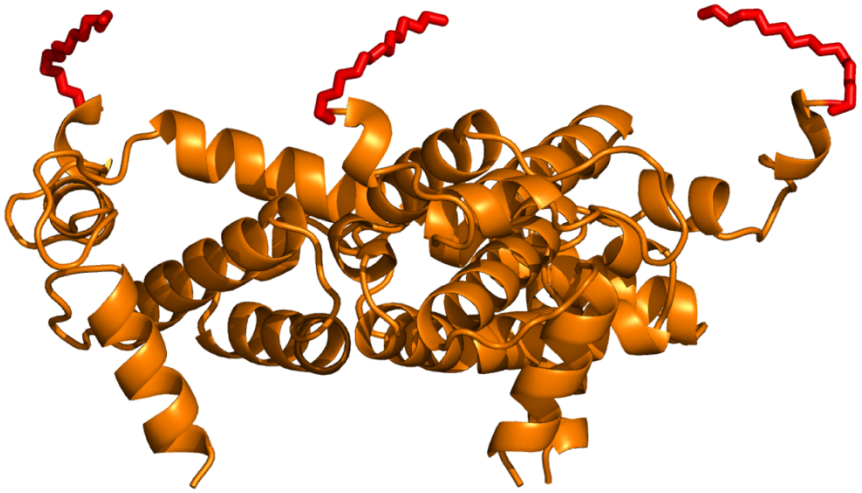

Figure S3. Structure of the myrMA$_{112}$ trimer with the myr group exposed. Cartoon representation of myrMA$_{112}$ trimer **b** with the myr group extruded. The dimer partner involved in myr swapping is not shown. The myr group is shown as a red stick.

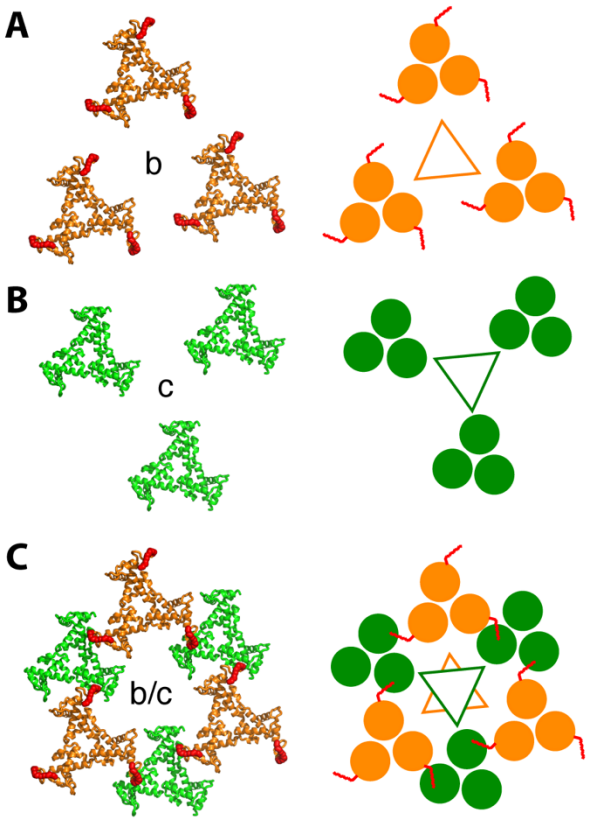

Figure S4. Organization of the myrMA$_{112}$ molecules in the crystal unit. (A) Trimers formed by chain **b** as spatially arranged in the crystal lattice with myr groups shown in red. Schematic representation illustrating the trimer lattice is shown in orange. (B) Arrangement of chain **c** trimers in the crystal lattice. The center of mass is identical to that shown for (A). (C) Hexamer of trimer lattice formed by packing of **b** and **c** chain trimers. Lattice formation yielded a central hole implicated in accommodation of the gp41CT domain of Env. In this lattice, the myr group is extruded and projecting out-of-plane. All six trimers are in a parallel mode with a three-fold rotation axis, with the N termini of each monomer in the foreground of the image.

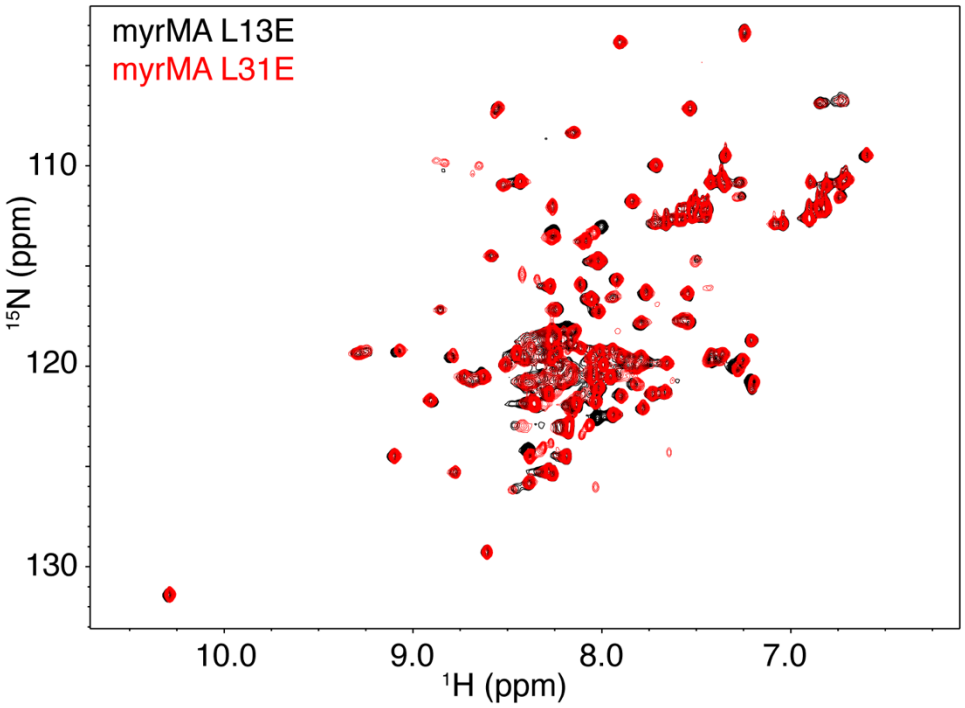

Figure S5. NMR spectra of myrMA mutants. Overlay of 2D ^{1}H-^{15}N HSQC spectra for myrMA L13E (black) and L31E (red) at 120 μM (308 K) in a buffer containing 50 mM sodium phosphates (pH 5.5), 100 mM NaCl, 1 mM EDTA, and 2 mM TCEP. The spectra are nearly identical, suggesting that the mutations induce very similar structural changes in the myrMA protein.

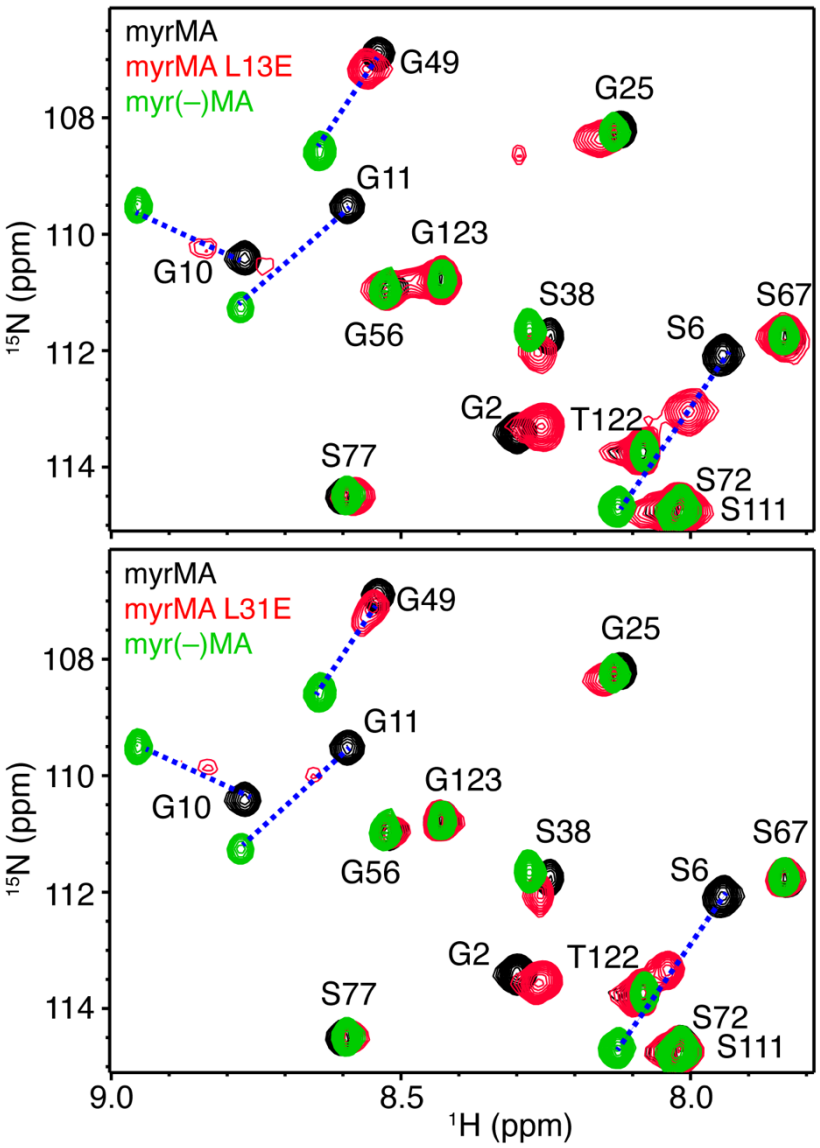

Figure S6. NMR spectra of WT and mutant myrMA. Overlay of 2D ^{1}H-^{15}N HSQC spectra for WT (black), myrMA L13E or L31E mutants (red), and myr(–)MA (green) at 120 μM in a buffer containing 50 mM sodium phosphates (pH 5.5), 100 mM NaCl, 1 mM EDTA, and 2 mM TCEP. For the myrMA L13E and L31E proteins, a subset of ^{1}H-^{15}N resonances shifted toward the corresponding signals of myr(–)MA, indicating a shift in equilibrium towards the myr–exposed state.

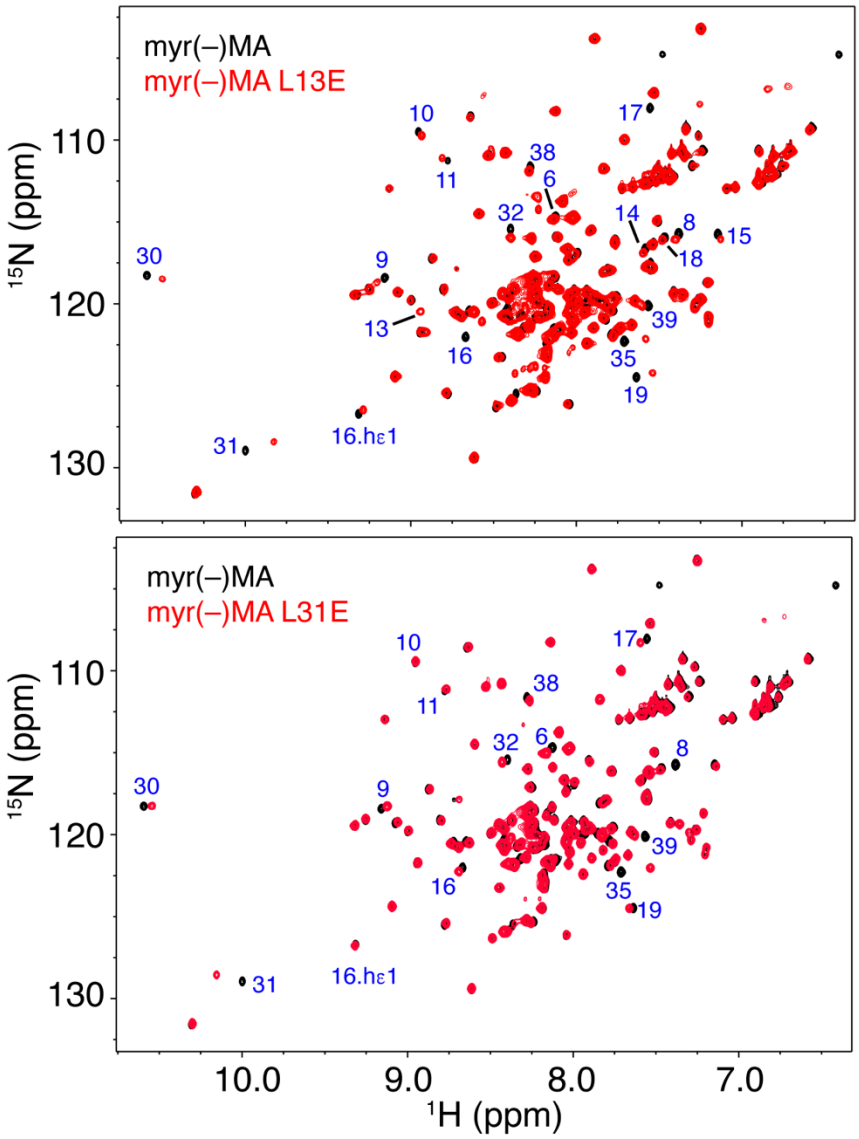

Figure S7. Comparison of NMR spectra of WT and mutant myr(–)MA. Overlay of 2D ^{1}H-^{15}N HSQC spectra for WT (black) and mutant (L13E and L31E; red) myr(–)MA proteins collected at 120 μM in a buffer containing 50 mM sodium phosphates (pH 5.5 or 6.0), 100 mM NaCl, 1 mM EDTA and 2 mM TCEP. A subset of ^{1}H-^{15}N resonances corresponding to residues in the N-terminal loop and helices I-II exhibited significant chemical shift changes or severe broadening, indicating a conformational change in these motifs.

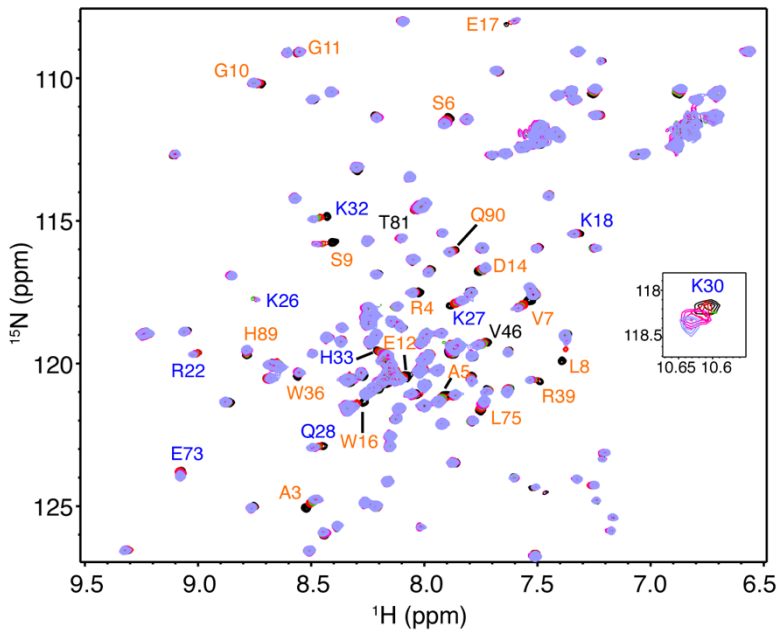

Figure S8. NMR data of IP_3 binding to myrMA. Overlay of 2D ^{1}H-^{15}N HSQC spectra upon titration of HIV-1 myrMA with IP_3 [60 μM, 35 °C; IP_3:myrMA = 0:1 (black), 1:1 (red), 2:1 (green), 4:1 (magenta) and 8:1 (slate)] in 50 mM phosphates (pH 5.5) and 2 mM TCEP. A subset of ^{1}H-^{15}N resonances corresponding to the IP_3 binding site are indicated by blue labels. A second subset of ^{1}H-^{15}N resonances shifted toward the corresponding signals of myr(–)MA (orange labels), indicating that IP_3 binding to myrMA caused a shift in equilibrium towards the myr– exposed state.

References

1. C. P. Hill, D. Worthylake, D. P. Bancroft, A. M. Christensen, W. I. Sundquist, Crystal Structures of the Trimeric HIV-1 Matrix Protein: Implications for Membrane Association. *Proc. Natl. Acad. Sci.* **93**, 3099-3104 (1996).